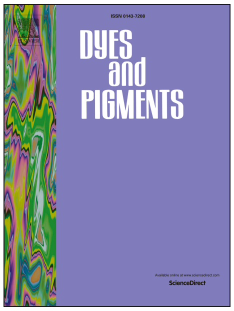

D-π-A-type aryl dialkylsulfonium salts as one-component versatile photoinitiators under UV/visible LEDs irradiation

Xingyu Wu, Jean-pierre Malval, Decheng Wan, Ming Jin

PII: S0143-7208(16)30125-5

DOI: 10.1016/j.dyepig.2016.04.004

Reference: DYPI 5182

To appear in: *Dyes and Pigments*

Received Date: 24 February 2016

Revised Date: 25 March 2016

Accepted Date: 1 April 2016

Please cite this article as: Wu X, Malval J-p, Wan D, Jin M, D-π-A-type aryl dialkylsulfonium salts as one-component versatile photoinitiators under UV/visible LEDs irradiation, *Dyes and Pigments* (2016), doi: 10.1016/j.dyepig.2016.04.004.

Graphical Abstract

One-component photoinitiators can initiate different photopolymerizations under soft irradiation conditions (365–450 nm LEDs)

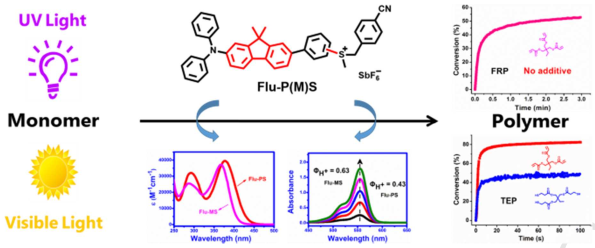

D-π-A-type aryl dialkylsulfonium salts as one-component versatile photoinitiators under UV/visible LEDs irradiation

Xingyu Wu,[a] Jean-pierre Malval,[b] and Decheng Wan,[a] Ming Jin*[a]

[a]*School of Materials Science and Engineering, Tongji Univsersity, 4800 Caoan Road, Shanghai, 201804, P.R. China.*

[b]*Institute de Science des Matériaux de Mulhouse, UMR CNRS 7361, Université de Haute-Alsace, 15 Rue Jean Starcky, Mulhouse, 68057, France.*

** Corresponding author. Tel.:+86-21-65980143*

E-mail address: mingjin@tongji.edu.cn

Abstract

Two D-π-A-type aryl dialkylsulfonium salts with substituted-fluorene as a conjugated system were developed as one-component, versatile photoinitiators under soft irradiation conditions (365–450 nm Light-emitting diodes). The mechanisms for photochemical generation of reactive species (cations and radicals) by the photoinitiators were studied by UV-Vis spectroscopy, theoretical calculations, fluorescence spectroscopy and cyclic voltammetry techniques. The high quantum yields for acid generation (Φ_H^+ = ~0.43 to 0.63) of the compounds enable the cationic polymerizations of epoxides and vinyl ether to proceed effectively. Meanwhile, the photocleavage products of sulfoniums (i.e., radicals) initiate the free radical polymerization of acrylate. Such versatile properties allowed them to serve as effective photoinitiators for the synthesis of interpenetrated polymer networks and thiol-ene polymerization without any co-initiators or additives. Based on their beneficial features, these photoinitiators hold great promise for use in photocuring applications.

Keywords: Photopolymerization; Sulfonium Salts; Photoinitiating Systems; One-component; Light-emitting diodes.

1. Introduction

Photopolymerization has aroused great interest due to its wide applicability in the manufacturing of coatings, adhesives, inks, and microelectronics; in 3D microfabrication; and so on.[1-6] Free radical polymerizations (FRP),[7] cationic polymerizations (CP),[8] cationic/radical copolymerizations for the syntheses of interpenetrated polymer networks (IPN)[9] and thiol-ene polymerizations (TEP)[10] are typical and well-known photopolymerization reactions for the formation of highly cross-linked networks that are utilized in different photocuring fields.[6] The search for efficient, versatile photoinitiator systems (PISs) which perform a concomitant radical/cationic dual curing in a one-step procedure upon excitation in the UV-Visible range should be highly useful for the development of new photopolymerization reactions.[11] Many multi-component mixtures (photoinitiators/coinitiators) are good versatile PISs and have been described in recent years.[12-16] Although the presence of co-initiators has always increased the efficiency of the initiating process, many additional problems also emerged. Most co-initiators are toxic and mutagenic, they tend to induce substrate corrosion, and cause cured films to yellow, all of which greatly limit their application, and one-component photoinitiators show special advantages.[17] Recently, Lalevee et al. reported iodonium-polyoxometalate and thianthrenium-polyoxometalate as one-component UV photoinitiators for radical and cationic polymerization through an intramolecular electron transfer from the counter anions to onium salts and exhibited higher reactivity.[18] Meanwhile, inspiring from the technological advances of light-emitting diodes (LEDs), PISs have been adapted to operate under LED irradiations, especially Near UV/visible LEDs.[19, 20] These eco-friendly PISs exhibit many advantages including low cost,[21] a lack of harmful UV, and a higher operating efficiency. Therefore, the use of one-component and versatile photoinitiators with long wavelength absorption would be of significant benefit to industrial applications that require photocuring.

Sulfonium salts have generated interest in the microelectronics field for its use as a photoacid generator (PAG)—a species that produces H^+ upon irradiation—in both positive- and negative-tone photoresist formulations.[2] In particular, sulfonium salts with non-nucleophilic anions such as PF_6^-, AsF_6^-, or SbF_6^- have found widespread use as photoinitiators for the cationic photopolymerizations of epoxides and vinyl ethers.[22, 23] The development of new sulfonium salts, with a suitable absorption wavelength and high performance, has been extensively explored.[24-27] The versatility of PAG photoinitiators is greatly limited because sulfonium salts are mainly confined to cationic polymerizations by H^+ production. However, as presumed from the photocleavage mechanism, the homolytic cleavage of the S-C bond leads to the formation of a cation-radical, on the sulfur-containing fragment, and a neutral radical; because this action occurs prior to the generation of H^+, it offers the possibility of initiating a radical polymerization.[6]

Herein, two novel D-π-A-type aryl dialkylsulfonium salts (Flu-PS and Flu-MS in Scheme 1) with substituted fluorenyl group as the π-conjugated system are designed and synthesized. In these two compounds, the fluorene unit exhibited a planar geometry, where a strong electron delocalization was expected,[28] thus, extending the absorption of sulfonium salts to match UV-Visible LEDs irradiation. Both sulfonium salts showed high efficiency and excellent photoacid generation (Φ_H^+ = 0.43 to ~0.63) and decomposed very rapidly under irradiation of 365–450 nm LEDs. The mechanism and production of reactive species (i.e., radicals and cations) were studied using UV-Vis spectroscopy, theoretical calculations, steady state photolysis, NMR, fluorescence, and cyclic voltammetry and electron spin resonance spin trapping techniques. Their roles as one-component (without any additives) versatile photoinitiators for FRP, CP, IPN, and TER were confirmed by real-time FT-IR upon exposure of Near UV or blue LEDs (365 – 450 nm) at low light intensities (1~4 mW cm^{-2}). The good wavelength tunability, high sensitivities, and economy, including high efficiency (1.0% additive), low excitation energy (1–4 mW cm^{2}, LEDs@365–405 nm) and one-component, make them useful and advantage for versatile photopolymerizations.

2. Experimental section

2.1 Materials

The PAGs and monomers investigated here are presented in Scheme 1 and used with the best purity available. N-vinylcarbazole (NVK), cyclohexene oxide (CHO), triethyleneglycol divinyl ether (DVE-3), methyl diethanolamine (MDEA), trimethylolpropane tris(3-mercaptopropionate) (Trithiol), trimethylolpropane triacrylate (TMPTA) and (3,4-Epoxycyclohexane)methyl 3,4-epoxycyclohexylcarboxylate (EPOX) were purchased from Sigma-Aldrich or J&K Chemical and used as received without further purification. All chemicals for synthesis were purchased from Sinopharm Chemical Reagent Co., Ltd.; TCI; or J&K Chemical, and they were used without further purification unless otherwise specified. All solvents employed for photophysical measurements were J&K Chemical spectroscopic grade.

2.2 General instrumentations

^{1}H NMR and ^{13}C NMR measurements were recorded with a Bruker 400M NMR spectrometer and chemical shifts were reported in parts per million (ppm) downfield from the Me_4Si resonance, which was used as the internal standard when recording NMR spectra. Elemental analysis was performed by Elementar Vario El III (Germany). Mass spectra were recorded on a Micromass GCTTM.

UV-Vis spectra were recorded on a Mapada UV-6300 spectrophotometer. The photodecomposition processes in a solution of acetonitrile and CHO were studied by UV-Vis spectra under an LED irradiation of 365 nm. Steady-state fluorescence spectra were collected using a Hitachi-2700 spectrofluorometer. Emission spectra were spectrally corrected.

Quantum yields for acid generation were measured under irradiation at 365 nm using LED point curing (Uvata, Shanghai). Both irradiated PAGs dissolved in acetonitrile were previously N_2-degassed. The progress of the photoreaction was monitored via UV-Vis absorption spectra. The absorbance at the excitation wavelength was greater than 2.5 to assume a total absorption of the incident photons. The dose rates were maintained sufficiently small so that the changes of A_λ were lower than 10%. Rhodamine B (RhB) was used as a sensor of photoacid generation.[29] The acid generation in acetonitrile was also evaluated from a calibration curve of RhB, which was gradually protonated by the addition of p-toluenesulfonic acid. The incident light intensity was measured by ferrioxalate actinometry.

Molecular orbital calculations were performed using the GAUSSIAN 09 package.[30] The electronic absorption spectra for different compounds were determined by time-dependent density functional theory (DFT) at the B3LYP/6-31G*. The molecular orbitals involved in these transitions could be extracted, and the geometries were frequency checked.

The cyclic voltammetry experiments (using a computer-controlled Radiometer Voltalab 6 potentiostat with a three-electrode single-compartment cell. The working electrode was a platinum disk, and a saturated calomel reference electrode (SCE) was placed in a separate compartment containing the supporting electrolyte and connected by a salt bridge) were performed at 300 K, in N_2-degassed acetonitrile with a constant concentration (0.1 M) of $(n\text{-Bu})_4NBF_4$. Ferrocene (Fc) was used as an internal reference (considering $E_{Fc/Fc+} = 0.53$ V in ACN vs. aqueous SCE).[24]

The photopolymerization was monitored in situ by Fourier transform real-time infrared spectroscopy (FT-RTIR) with a Nicolet iS5 spectrometer. The evolution of the epoxy group content in EPOX and CHO, the double bond content of TMPTA and DVE-3, and the thiol (S-H) content of Trithiol were continuously followed by real time FTIR spectroscopy at approximately 790, 780, 1630, 1620 and 2580 cm^{-1}, respectively.[14, 31]

2.3 Synthesis

The synthetic route of PAGs are shown in Scheme 2, and the details of characterization are provided in the electronic supporting information (ESI†).

*2.3.1 Preparation of 2-bromo-7-N,N'-diphenylamino-9,9'-dimethyl-9H-fluorene (**1**)*

2,7-dibromo-9,9'-dimethyl-*9H*-fluorene (25.5 g, 72.31 mmol) was added to a mixture of diphenylamine (12.2 g, 72.31 mmol), Cu powder (2.0 g, 31.25 mmol), potassium carbonate (20.0 g, 0.14 mol) and 18-crown-6 (2.0 g, 8.33 mmol) in 1,2-dichlorobenzene (30 mL) under nitrogen atmosphere at room temperature. The resultant mixture was stirred for 10 min and then refluxed at 200 °C for 24 h. Then, the reaction mixture was cooled to room temperature, the 1,2-dichlorobenzene was distilled at low pressure and the mixture was extracted three times with CH_2Cl_2 (3 × 150 mL). The product was purified by column chromatography with use of 2% ethyl acetate in hexanes as eluent to give 25.2 g of colorless solid (79.0%). ^{1}H NMR (400 MHz, $CDCl_3$): δ 7.53–7.41 (m, 4H), 7.28–7.24 (m, 4H), 7.16–7.12 (m, 5H), 7.04–6.99 (m, 3H), 1.39 (s, 6H).

*2.3.2 Preparation of 9,9'-dimethyl-2-(3-methylthio)phenyl-7-N,N'-diphenylamino-9H-fluorene (**Pre-M**) and 9,9'-dimethyl-2-(4-methylthio)phenyl-7-N,N'-diphenylamino-9H-fluorene (**Pre-P**)*

A mixture of 1 (5.0 g, 11.4 mmol), 3-(methylthio)phenylboronic acid or 4-(methylthio)phenylboronic acid (2.1 g, 11.4 mmol), potassium carbonate (4.7 g, 34.2 mmol), $Pd(PPh_3)_4$ (0.7 g, 0.6 mmol) and methyl trioctyl ammonium chloride (2.0 mL) in toluene (40 mL), ethanol (24 mL) and water (8 mL) was stirred under N_2 atmosphere at 100 °C for 24 h. The resulting solution was cooled to room temperature, extracted with dichloromethane (3 × 100 mL), washed with water and dried over anhydrous $MgSO_4$. The crude product was purified by column chromatography on silica gel using dichloromethane/petroleum ether (1:5, v/v) as eluent to afford the desired product as a white solid.

Pre-M: 4.5 g, 82.3%. ^{1}H NMR (400 MHz, $CDCl_3$): δ 7.68 (d, *J* = 7.8 Hz, 1H), 7.59–7.52 (m, 4H), 7.43–7.35 (m, 2H), 7.28–7.23 (m, 5H), 7.20 (s, 1H), 7.15–7.13 (m, 4H), 7.04–7.01 (m, 3H), 2.55 (s, 3H), 1.45 (s, 6H). ^{13}C NMR (101 MHz, $CDCl_3$): δ 155.4, 154.3, 148.0, 147.5, 142.4, 139.0, 138.6, 133.6, 129.3, 126.3, 125.6, 125.2, 124.2, 123.3, 122.8, 121.3, 120.8, 119.8, 118.5, 47.0, 27.2, 16.1. MS: m/z 484.20 [M + H^+] (Calcd. for $C_{34}H_{29}NS$: 483.20). Anal. Calcd. (%) for $C_{34}H_{29}NS$: C, 84.43; H, 6.04; N, 2.90; Found: C, 84.59; H, 6.07; N, 2.68.

Pre-P: 4.3 g, 80.2%. ^{1}H NMR (400 MHz, $CDCl_3$): δ 7.65 (s, 1H), 7.58 (m, 4H), 7.52 (d, *J* = 7.9 Hz, 1H), 7.36–7.33 (m, 2H), 7.29–7.25 (m, 5H), 7.14–7.13 (m, 5H), 7.02 (m, 2H), 2.53 (s, 3H), 1.45 (s, 6H). ^{13}C NMR (101 MHz, $CDCl_3$): δ 155.3, 154.3, 148.0, 147.4, 138.8, 138.5, 138.3, 137.3, 133.7, 129.3, 127.5, 127.1, 125.9, 124.2, 123.3, 122.7, 121.0, 120.7, 119.8, 118.5, 47.0, 27.2, 16.1. MS: m/z

484.20 [M + H$^+$] (Calcd. for $C_{34}H_{29}NS$: 483.20). Anal. Calcd. (%) for $C_{34}H_{29}NS$: C, 84.43; H, 6.04; N, 2.90; Found: C, 84.49; H, 5.97; N, 2.78.

*2.3.3 Preparation of **Flu-MS** and **Flu-PS***

In a dark room, precursors (500.0 mg, 1.03 mmol), silver trifluoromethanesulfonate (529.0 mg, 2.06 mmol) and Cs_2CO_3 (672.0 mg, 2.06 mmol) were added to anhydrous CH_2Cl_2 (30 mL) under N_2 atmosphere at room temperature. Then, 4-cyanobenzyl bromide (403.8 mg, 2.06 mmol) dissolved in 5 mL of anhydrous CH_2Cl_2 was syringed in half hour. The mixture was stirred for 48 h in the dark. Then, the crude products were directly purified by column chromatography on silica gel using chloroform/methanol (10:1, v/v) as eluent to afford the desired product as a yellow solid. The product was used in the ion-metathesis described below without further purification. A fresh 50 mL portion of aqueous $NaSbF_6$ (4.60 g, 25.0 mmol) was added to a solution of prepared PAGs in 20 mL of acetone. The mixture was stirred for 2 h at room temperature in the dark. The solid was collected by filtration and re-dissolved in 10 mL of acetone. The above anion-exchange was repeated three times and gave the final products.

Flu-MS: 575.3 mg, 75.0%. ^{1}H NMR (400 MHz, CD_3CN): δ 8.06 (s, 1H), 8.00 (s, 1H), 7.76–7.58 (m, 9H), 7.43–7.41 (m, 2H), 7.28–7.22 (m, 4H), 7.05–7.00 (m, 6H), 6.94 (d, J = 8.2 Hz, 1H), 5.06 (d, J = 12.7 Hz, 1H), 4.88 (d, J = 12.7 Hz, 1H), 3.32 (s, 3H), 1.42 (s, 6H). ^{13}C NMR (101 MHz, CD_3CN) δ: 155.4, 154.3, 147.5, 143.6, 139.3, 135.8, 132.9, 132.7, 132.3, 131.3, 131.0, 129.1, 128.7, 128.3, 126.1, 123.9, 122.8, 122.6, 122.2, 121.2, 121.0, 119.8, 117.7, 117.5, 117.0, 113.3, 49.7, 46.5, 25.9, 24.1. MS: m/z 599.25 [sulfonium ion] (Calcd. for $C_{42}H_{35}N_2S^+$: 599.25). Anal. Calcd. (%) for $C_{42}H_{35}F_6N_2SSb$: C, 60.37; H, 4.22; N, 3.35; Found: C, 60.57; H, 4.07; N, 3.68. Decomposition before melting and the thermal decomposition temperature (T_d, temperature at 5% weight loss in TGA): 147.5 ^oC.

Flu-PS: 590.0 mg, 78.0%. ^1H NMR (400 MHz, CD_3CN): δ 7.99–7.97 (m, 2H), 7.83–7.66 (m, 9H), 7.38–7.20 (m, 7H), 7.12–7.03 (m, 6H), 4.92 (d, *J* = 12.8 Hz, 1H), 4.74 (d, *J* = 12.8 Hz, 1H), 3.23 (s, 3H), 1.43 (s, 6H). ^{13}C NMR (101 MHz, CD_3CN) δ: 155.5, 154.4, 147.8, 147.5, 147.3, 139.7, 135.8, 132.8, 132.4, 132.2, 131.2, 131.0, 129.1, 128.6, 126.3, 123.9, 122.8, 122.5, 121.4, 121.0, 119.9, 119.1, 117.7, 117.6, 117.0, 113.3, 49.9, 46.6, 25.8, 24.4. MS: m/z 599.25 [sulfonium ion] (Calcd. for $C_{42}H_{35}N_2S^+$: 599.25). Anal. Calcd. (%) for $C_{42}H_{35}F_6N_2SSb$: C, 60.37; H, 4.22; N, 3.35; Found: C, 60.61; H, 4.37; N, 3.57. Thermal decomposition temperature (T_d): 184.0 ^oC.

3. Results and discussion

3.1 Synthesis

Two sulfonium salts, Flu-PS and Flu-MS, were prepared from 2,7-dibromofluorene in four steps (Scheme 2). Cu-catalyzed coupling with diphenylamine produced the triphenylamine-containing conjugated system because the triphenylamine group has been proven as a good substituent in sulfonium salts.[32] Then, Suzuki reactions were performed with para/meta-(methylthio)-phenylboronic acid to produce the precursors in high yield (over 80%). Finally, alkylation of the precursors with 4-cyanobenzyl bromide and $AgCF_3SO_3$ gave fluorene-containing sulfonium triflate salts; then, non-nucleophilic anions, such as SbF_6^-, were exchanged to benefit the polymerization reactions.[32]

3.2 Photochemical and photophysical properties of the sulfonium salts

The absorption spectra of the two sulfonium salts (Flu-MS and Flu-PS) in acetonitrile are shown in Fig. 1. The maxima for Flu-MS and Flu-PS are located in the UV-Vis at λ_{max} = 368 nm ($\varepsilon_{368\ nm}$ ~ 36,900 M^{-1} cm^{-1}) and λ_{max} = 378 nm ($\varepsilon_{378\ nm}$ ~ 39,400 M^{-1} cm^{-1}), respectively (see Table 1). As to the spectrum of Flu-PS, it presents a slight redshift and a higher ε value due to its stronger conjugated effect.[24] The excellent absorption properties of PAGs are associated with the large delocalization of the highest occupied molecular orbital (HOMO) and the lowest unoccupied molecular orbital (LUMO), which are involved in the lowest energy transitions.[24, 33] This result is further confirmed by DFT calculations, as shown in Fig. 2. The HOMOs of sulfoniums are mainly localized on the triphenylamine (donor) and fluorene (conjugated system) moieties; however, the LUMOs are chiefly distributed throughout the sulfonium moieties. Saeva has proved that for arylsulfonium salts, the photoreaction can happen either by direct excitation of a π-σ* (sulfur-carbon bond) transition or by excitation of a π-π* transition, which is followed by intramolecular electron transfer to the σ* on sulfur-carbon bond.[34-36] In both cases, subsequent homolytic cleavage of the S-C bond leads to the formation of a radical cation on the sulfur-containing fragment and a neutral radical on the carbon fragment. The results obtained from the theoretical calculations confirm that the S-C σ* bond (face to face) does exist in the LUMO orbitals of both PAGs, as shown in Fig. 2.

The typical evolution of the absorption spectra of Flu-MS in acetonitrile, upon irradiation by 365 nm LED, is shown in Fig. 3(a). While the band located at approximately 280 nm increases slightly, the maximum-wavelength absorption band dramatically collapses with the appearance of a less intensive band located at 356 nm. Moreover, upon photolysis, a highly fluorescent byproduct is progressively generated (Fig. S1, ESI†). The excitation spectrum recorded at the maximum fluorescence wavelength matches perfectly with the absorption spectrum of the precursor (Pre-M), which presents a distinctive band at 360 nm (Fig. S2, ESI†). In addition, this effect is corroborated by the slight increase of the absorption band of Pre-M (λ_{max} at 365 nm) when the photolysis of Flu-MS is performed as the monomer, i.e., CHO, as shown in Fig. 3(b).

The photolysis of Flu-MS is also confirmed by ^{1}H NMR spectra upon irradiation in $CDCl_3$ (Fig. S3(a), ESI†). The evolution of the proton signals proves the decomposition of Flu-MS. At the same time, the single peaks located from 3 to ~5 ppm indicate the coupling of the 4-cyanobenzyl radical with the molecular framework.[37] When 10 eqv. of CHO was co-photolyzed with Flu-MS, the produced H^+ can initiate the polymerization of CHO and the byproducts are being compared. ^{1}H NMR shows signals of the polymerization of CHO (Fig. S3b and 3c, ESI†). Interestingly, the ^{1}H NMR analyses also indicate that the yield for generation of Pre-M is strongly increased when the photolysis is performed in CHO (Fig. S3(b), ESI†) due to fewer and weaker single peaks appearing at approximately 4–5 ppm. Note that the same effects are observed for Flu-PS, as displayed in Fig. S1 and Fig. S4 (ESI†). Similar to the mechanism established for aryl sulfonium salts,[34] we proposed that the photogeneration of acids mainly stems from an intramolecular rearrangement initiated by a photoinduced electron transfer (PET) from the amino group to sulfonium; and the possible hydrolysis mechanism are shown in Scheme 3. As previously demonstrated,[32] this PET process is supported by the estimation of the corresponding free energy change (ΔG_{eT}) using the Rehm−Weller equation [eq (1)]. In this formula, E_{ox} and E_{red} correspond to the oxidation and reduction potentials of the donor and acceptor, respectively. E_{00} is the energy of the singlet excited state, which is calculated by Berlman’s method.[38] C is the Coulombic energy term characterizing the interaction of the radical-ion pairs. In acetonitrile, this term usually makes a small contribution to the overall energy change for PET and is neglected in the calculation, as was previously assumed for other sulfonium-based derivatives.[34, 37]

$$\Delta G_{eT} = E_{ox} - E_{red} - E_{00} - C \qquad (1)$$

The values of E_{ox} and E_{red} are determined from cyclic voltammetry (Fig. 4 and Fig. S5, ESI†) The sulfonium salts exhibit an irreversible electrochemical reduction wave with a single peak at -1.1 V and -1.2 V vs. SCE for Flu-MS and Flu-PS, respectively. These cathodic potentials should be assigned to the one-electron reduction of the sulfonium group.[36] The energy of the excited singlet state, E_{00}, was obtained from the wavelength at the intersection of the normalized absorption and emission spectra; the values were estimated to be 3.02 eV and 2.88 eV for Flu-MS and Flu-PS, respectively. Table 1 summarizes the free energy changes associated with the electron transfer (ΔG_{eT}) in the PAGs, which are thermodynamically favorable. This indicates that there is a large driving force for electron transfer ($\Delta G_{eT} < -100$ kJ mol^{-1} for Flu-MS) from the first excited singlet state.

Then, the quantum yields of H^+ generation were monitored at 365 nm irradiation (Table 1). It can be observed that the Φ_{H^+} of Flu-PS is 0.43. Interestingly, Flu-MS shows a higher Φ_{H^+} of 0.63 at 365 nm irradiation. The high acid generation quantum yields of the fluorene-containing sulfonium salts reported here show that dissociation is energetically favorable, i.e., $\Delta G_{eT} < -100$ kJ mol^{-1}, which is higher than the triphenylamine-based sulfonium salts without the conjugated systems as reported by Perry and Marder ($\Delta G_{eT} = -85.3$ kJ/mol, $\Phi_{H^+} = 0.48$) [32]. These results suggest that the electron donating ability of the diphenylamine strongly activates the dissociation of the S-C bond by stabilizing the triphenylamine-fluorene methyl sulfide cation species, as shown in Scheme 3, such that the total product energy now favors the dissociation from the π-σ^* excited state. In addition, the stability of a 4-cyanobenzyl radical also favors the dissociation. [24]

3.3 Photoinitiating ability of the sulfonium salts

a. The cationic photopolymerizations of epoxides and vinyl ether. The photopolymerizations of EPOX, CHO and DVE-3 in the presence of the two sulfonium salts (1 wt%) and in air, were carried out using 365 nm to 450 nm LEDs exposure because the two initiators showed considerable extinction coefficients in this range (Table 2). Both of the sulfonium salts can initiate the polymerizations of three monomers and the conversion profiles for these reactions are depicted in Fig. 5, Fig. S6 and S7 (ESI), and their conversions at t = 3 min are summarized in Table 3 and Table S1 (ESI). At 365 nm, Flu-MS shows faster conversions than Flu-PS (initial parts of curves) for all monomers (Fig. 5) ascribing to the higher Φ_{H^+}. The conversions of DVE-3 are nearly 100% (Table 3) for both sulfonium salts and the conversions of CHO reach 79~85%. The conversions of EPOX are relatively lower than DVE-3 and CHO but also can arrive at 70% for Flu-MS. Upon 385 to 450 nm irradiation, the conversions are similar at same light intensity (Fig. S6, S7 and Table S1, ESI). In line with the behaviour of other sulfonium salts cationic photoinitiators, reactions r_1-r_3 account for the generation of H^+ by the two sulfoniums [26, 27] (Scheme 3) and initiate the polymerizations.

b. The free radical photopolymerization of acrylates. Flu-MS and Flu-PS enable the free radical polymerization (FRP) of TMPTA in laminate upon exposure to 365, 385 and 405 nm LEDs at low intensity (4 mW cm^{-2}) (Fig. 6, Table 3, and Table S1). Curves for Flu-MS exhibit conversions from 58% to 43% for 365 nm to 405 nm, while curves for Flu-PS give nearly stable conversions over the same spectral range (~60%). It is concluded that Flu-PS is better than Flu-MS at initiating FRP. A comparison of the Flu-MS/MDEA system with Flu-MS itself under soft irradiation (1 mW cm^{-2}, Fig. 6) shows that Flu-MS has an induction time, whereas MDEA can reduce the induction time efficiently.[1]

c. On the IPN synthesis: photopolymerization of EPOX/TMPTA blends. A simultaneous cationic/radical photopolymerization of an EPOX/TMPTA blend (50%/50% w/w) using the Flu-PS or Flu-MS is feasible, as well (formation of an interpenetrated polymer network, Fig. 7). The final conversions of TMPTA and EPOX are both higher in laminate than in air (Table 3 and Table S1), and Flu-PS exhibits higher conversions than Flu-MS. It is interesting to find that conversions of TMPTA is greater when blended (70%) than in single monomer systems (56%), which suggests a synergistic effect in the IPN synthesis.

d. In Thiol-Ene photopolymerization. Flu-MS and Flu-PS are also capable of initiating a fast thiol-ene (Trithiol/TMPTA) polymerization (r_4-r_6) with a 365 nm LED exposure at low light intensity, i.e., 2 mW cm^{-2} (Fig. 8). After ~10 s of light irradiation, the vinyl double bond of TMPTA and the thiol (−SH) group of Trithiol arrive at their maximum conversions (80% and 42%, respectively). The difference in ultimate conversion efficiency between the vinyl double bond and −SH (82.4% and 49.7% after 60 s of light exposure, Table 3) suggests a significant contribution to the free radical polymerization through the self-initiation of TMPTA.

$$M^{\bullet} + RS\text{-}H \rightarrow M\text{-}H + RS^{\bullet} \qquad (r_4)$$

$$RS^{\bullet} + R'\text{-}CH{=}CH_2 \rightarrow R'\text{-}CH^{\bullet}\text{-}CH_2SR \qquad (r_5)$$

$$R'\text{-}CH^{\bullet}\text{-}CH_2SR + RSH \rightarrow R'\text{-}CH_2\text{-}CH_2SR + RS^{\bullet} \qquad (r_6)$$

4. Conclusions

In conclusion, two new fluorene-containing D-π-A type sulfonium salts bearing a non-nucleophilic counterion, SbF_6^-, have been designed to be used as versatile photoinitiators. Key features of these sulfonium salts are that (i) they produce H^+ very efficiently upon exposure to 365–405 nm radiation and even to visible light, for example, λ > 400 nm for Flu-PS at very low intensity and (ii) the resulting Brønsted acid/radicals from the photolysis reactions initiate the versatile photopolymerizations without any additives, i.e., they can be used as one-component photoinitiators. Photochemically generated radicals and cations should be useful for photocuring highly viscous media or coatings, as well as for acid-activated material processing and fabrication in the solid phase. Finally, this approach suggests a new design strategy for the synthesis of very efficient sulfonium salts that could be excited over a broad spectral range by either single-photon or multiphoton excitation.

Acknowledgments

This work was supported by the National Natural Science Foundation of China (21273020, 51173134, 51573139); Fundamental Research Funds for the Central Universities and the Open Measuring Fund for Large Instrument and Equipment, Tongji University.

Appendix A. Supplementary data

Evolution of the UV-Vis spectra, emission spectra, On-line ^{1}H NMR spectra of sulfonium salts, cyclic voltammetry of Flu-PS, photopolymerization profiles of CHO and DVE-3 under different LED irradiations, and ^{1}H NMR and ^{13}C NMR of precursors and sulfonium salts.

References

[1] Fouassier JP. Photoinitiator, Photopolymerization and Photocuring: Fundamentals and Applications. Hanser Publishers: New York; 1995.

[2] Crivello JV. Photoinitiators for Free Radical, Cationic and Anionic Photopolymerization. 2nd Edition ed: John Wiley & Sons: Chichester; 1998.

[3] Dietliker K. A Compilation of Photoinitiators Commercially Available for UV Today. Sita Technology Ltd, Edinburgh, London; 2002.

[4] Green WA. Industrial Photoinitiators. CRC Press: Boca Raton; 2010.

[5] Fouassier JP, Lalevee J. Photoinitiator for Polymer Synthesis-Scope, Reactivity, and Efficiency. Wiley-VCH Berlag GmbH & Co. KGaA: Weinheim; 2012.

[6] Yagci Y, Jockusch S, Turro NJ. Photoinitiated Polymerization: Advances, Challenges, and Opportunities. Macromolecules. 2010;43(15):6245-60.

[7] Wang X, Jin, Zhang W, Tao X, Duan X-M, Jiang M. Novel D–π3–(A)1–3 multibranched chromophores as an efficient two-photon-induced polymerization initiator. Dyes Pigment. 2011;88(1):57-64.

[8] Crivello JV, Kong SQ. Synthesis and characterization of second-generation dialkylphenacylsulfonium salt photoinitiators. Macromolecules. 2000;33(3):825-32.

[9] Podsiadły R, Podemska K, Szymczak AM. Novel visible photoinitiators systems for free-radical/cationic hybrid photopolymerization. Dyes Pigment. 2011;91(3):422-6.

[10] Qin X-H, Torgersen J, Saf R, Muehleder S, Pucher N, Ligon SC, et al. Three-Dimensional Microfabrication of Protein Hydrogels via Two-Photon-Excited Thiol-Vinyl Ester Photopolymerization. J Polym Sci, Part A: Polym Chem. 2013;51(22):4799-810.

[11] Xiao P, Zhang J, Dumur F, Tehfe MA, Morlet-Savary F, Graff B, et al. Visible light sensitive photoinitiating systems: Recent progress in cationic and radical photopolymerization reactions under soft conditions. Prog Polym Sci. 2015;41:32-66.

[12] Durmaz YY, Moszner N, Yagci Y. Visible light initiated free radical promoted cationic polymerization using acylgermane based photoinitiator in the presence of onium salts. Macromolecules. 2008;41(18):6714-8.

[13] Podsiadly R, Strzelczyk R. N-substituted quinoxalinobenzothiazine/iodonium salt systems as visible photoinitiators for hybrid polymerization. Dyes Pigment. 2013;97(3):462-8.

[14] Xiao P, Hong W, Li Y, Dumur F, Graff B, Fouassier JP, et al. Green light sensitive diketopyrrolopyrrole derivatives used in versatile photoinitiating systems for photopolymerizations. Polym Chem. 2014;5(7):2293-300.

[15] Kabatc J, Jurek K. New two- and three-cationic polymethine dyes. Synthesis, properties and application. Dyes Pigment. 2015;112:24-33.

[16] Podsiadly R, Podemska K, Szymczak AM. Novel visible photoinitiators systems for free-radical/cationic hybrid photopolymerization. Dyes Pigment. 2011;91(3):422-6.

[17] Yang J, Tang R, Shi S, Nie J. Synthesis and characterization of polymerizable one-component photoinitiator based on sesamol. Photochem Photobiol Sci. 2013;12(5):923-9.

[18] Mokbel H, Xiao P, Simonnet-Jegat C, Dumur F, Gigmes D, Toufaily J, et al. Iodonium-Polyoxometalate and Thianthrenium-Polyoxometalate as New One-Component UV Photoinitiators for Radical and Cationic Polymerization. J Polym Sci, Part A: Polym Chem. 2015;53(8):981-9.

[19] Liu G, Zhu X, Xu B, Qian X, Song G, Nie J. Cationic photopolymerization of bisphenol A diglycidyl ether epoxy under 385 nm. J Appl Polym Sci. 2013;130(5):3698-703.

[20] Xiao P, Frigoli M, Dumur F, Graff B, Gigmes D, Fouassier JP, et al. Julolidine or Fluorenone Based Push-Pull Dyes for Polymerization upon Soft Polychromatic Visible Light or Green Light. Macromolecules. 2014;47(1):106-12.

[21] Dietlin C, Schweizer S, Xiao P, Zhang J, Morlet-Savary F, Graff B, et al. Photopolymerization upon LEDs: new photoinitiating systems and strategies. Polym Chem. 2015;6(21):3895-912.

[22] Pappas SP, Tilley MG, Pappas BC. Anthracene-bound sulfonium salts: highly efficient photoinitiators for cationic polymerization A new synthesis of sulfonium salts which avoids the use of silver salts. J Photochem Photobiol A-Chem. 2003;159(2):161-71.

[23] Cook WD, Chen S, Chen F, Kahveci MU, Yagci Y. Photopolymerization of Vinyl Ether Networks Using an Iodonium Initiator-The Role of Photosensitizers. J Polym Sci, Part A: Polym Chem. 2009;47(20):5474-87.

[24] Xia R, Malval J-P, Jin M, Spangenberg A, Wan D, Pu H, et al. Enhancement of Acid Photogeneration Through a Para-to-Meta Substitution Strategy in a Sulfonium-Based Alkoxystilbene Designed for Two-Photon Polymerization. Chem Mater. 2012;24(2):237-44.

[25] Jin M, Xu H, Hong H, Malval J-P, Zhang Y, Ren A, et al. Design of D-pi-A type photoacid generators for high efficiency excitation at 405 nm and 800 nm. Chem Commun. 2013;49(76):8480-2.

[26] Jin M, Hong H, Xie J, Malval J-P, Spangenberg A, Soppera O, et al. pi-conjugated sulfonium-based photoacid generators: an integrated molecular approach for efficient one and two-photon polymerization. Polym Chem. 2014;5(16):4747-55.

[27] Jin M, Wu X, Xie J, Malval JP, Wan D. One/two-photon-sensitive photoacid generators based on benzene oligomer-containing D-[small pi]-A-type aryl dialkylsulfonium salts. RSC Adv. 2015;5(68):55340-7.

[28] Jin M, Malval J-P, Versace D-L, Morlet-Savary F, Chaumeil H, Defoin A, et al. Two-photon absorption and polymerization ability of intramolecular energy transfer based photoinitiating systems. Chem Commun. 2008(48):6540-2.

[29] Pohlers G, Scaiano JC, Sinta R. A novel photometric method for the determination of photoacid generation efficiencies using benzothiazole and xanthene dyes as acid sensors. Chem Mater. 1997;9(12):3222-30.

[30] Frisch MJ. Gaussian 09, Revision B.01.: Gaussian, Inc: Wallingford CT. Wallingford CT2009.

[31] Zhang J, Frigoli M, Dumur F, Xiao P, Ronchi L, Graff B, et al. Design of Novel Photoinitiators for Radical and Cationic Photopolymerizations under Near UV and Visible LEDs (385, 395, and 405 nm). Macromolecules. 2014;47(9):2811-9.

[32] Zhou WH, Kuebler SM, Carrig D, Perry JW, Marder SR. Efficient photoacids based upon triarylamine dialkylsulfonium salts. J Am Chem Soc. 2002;124(9):1897-901.

[33] Jin M, Xie J, Malval J-P, Spangenberg A, Soppera O, Versace D-L, et al. Two-photon lithography in visible and NIR ranges using multibranched-based sensitizers for efficient acid generation. J Mater Chem C. 2014;2(35):7201-15.

[34] Saeva FD, Breslin DT, Luss HR. Intramolecular photoinduced rearrangements via electron-transfer-induced, concerted bond cleavage and cation radical/radical coupling. J Am Chem Soc. 1991;113(14):5333-7.

[35] Saeva FD, Garcia E, Martic PA. Comparative photochemical behavior of some anthracenyl and naphthacenyl sulfonium salt derivatives. J Photochem Photobiol A-Chem. 1995;86(1-3):149-54.

[36] Wang XZ, Saeva FD, Kampmeier JA. Photosensitized reduction of sulfonium salts: Evidence for nondissociative electron transfer. J Am Chem Soc. 1999;121(18):4364-8.

[37] Saeva FD, Morgan BP. Mechanism of one-electron electrochemical reductive cleavage reactions of sulfonium salts. J Am Chem Soc. 1984;106(15):4121-5.

[38] Berlman IB. Handbook of Fluorescent Spectra of Aromatic Molecules, 2nd ed.: Academic Press: New York; 1971.

Figure Captions.

Scheme 1 Chemical Structures of PAGs, monomers and additives.

Scheme 2 Synthetic route of the precursors and PAGs. a) Cu, K_2CO_3, 18-Crown-6, N_2, 200 °C, 24 h; b) K_2CO_3, $Pd(PPh_3)_4$, toluene, EtOH, water, 100 °C, 24 h; c) Cs_2CO_3, CH_2Cl_2, RT; d) $NaSbF_6$, water, acetone.

Scheme 3 Proposed photolysis mechanism of sulfoniums.

Fig. 1 The UV-Vis spectra of Flu-PS and Flu-MS in acetonitrile.

Fig. 2 Highest occupied molecular orbitals (HOMO) and lowest unoccupied molecular orbitals (LUMO) of Flu-M(P)S at B3LYP/6-31G(d) level.

Fig. 3 Evolution of the absorption spectra of Flu-MS in ACN (a) and in CHO (b) during irradiation at 365 nm (1 mW cm^{-2}).

Fig. 4 Cyclic voltammogram of Flu-MS in acetonitrile + $(n\text{-}Bu)_4NBF_4$ (0.1 M) on platinum electrode at 100 mV s^{-1}.

Fig. 5 Photopolymerization profiles of EPOX, CHO and DVE-3 under air in the presence of Flu-P(M)S (1 wt%) at 365 nm LED irradiation.

Fig. 6 Photopolymerization profiles of TMPTA in laminate in the presence of Flu-PS and Flu-MS (1 wt%) with LED illumination at 365, 385, and 405 nm (4 mW cm^{-2}); Flu-MS and Flu-MS/MDEA (1%/3%, w/w) with LED illumination at 365 nm (1 mW cm^{-2}); and Pre-P (1 wt%) with LED illumination at 365 nm (4 mW cm^{-2}).

Fig. 7 Photopolymerization profiles of a TMPTA/EPOX blend (50%/50%, w/w) in the presence of Flu-MS (a) and Flu-PS (b) (1 wt%) in laminate and under air, and with LED illumination at 365 nm (2 mW cm^{-2}).

Fig. 8 Photopolymerization profiles of Trithiol/TMPTA blend (50%/50%, w/w) in laminate in the presence of Flu-MS and Flu-PS (1 wt%) with LED illumination at 365 nm (2 mW cm^{-2}).

Table 1 Summary of optical data and electrochemical parameters for Flu-PS and Flu-MS.

Table 2 Light absorption properties of sulfoniums and their molar extinction coefficients (ε in M^{-1} cm^{-1}) at the maximum emission wavelengths of different LEDs.

Table 3 DVE-3, CHO, EPOX, TMPTA, TMPTA/EPOX and TMPTA/Trithiol conversions obtained with 365 nm LED illumination in the presence of Flu-MS or Flu-PS (1 wt%).

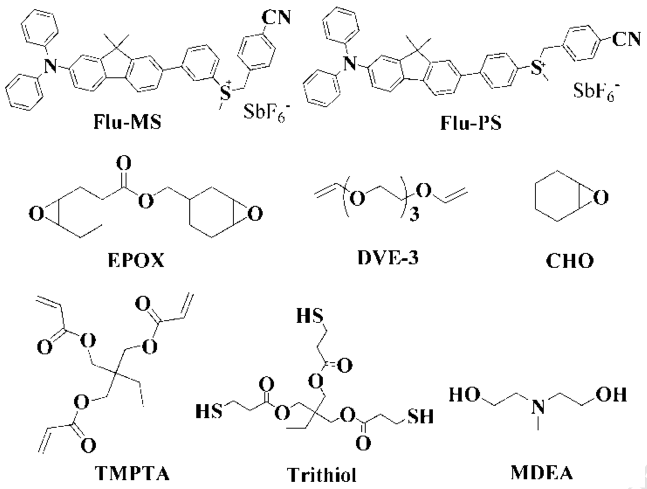

Scheme 1 By Ming JIN et al.

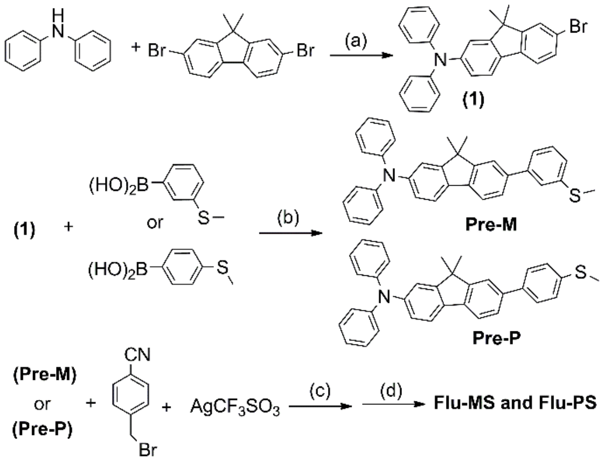

Scheme 2 By Ming JIN et al.

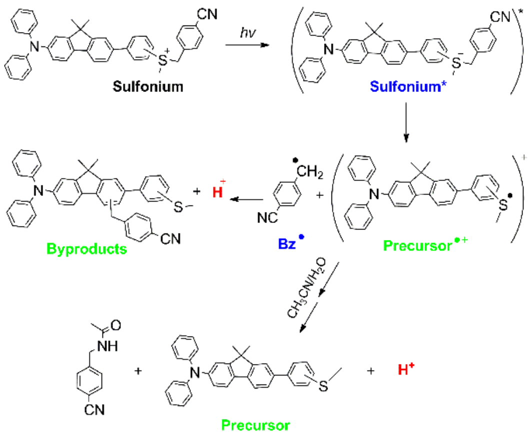

Scheme 3 By Ming JIN et al.

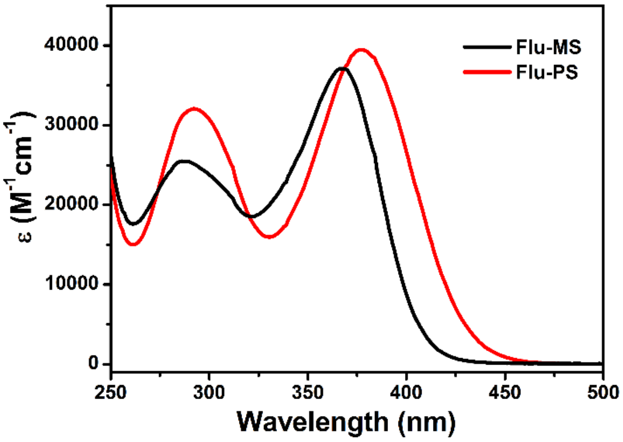

Fig. 1 By Ming JIN et al.

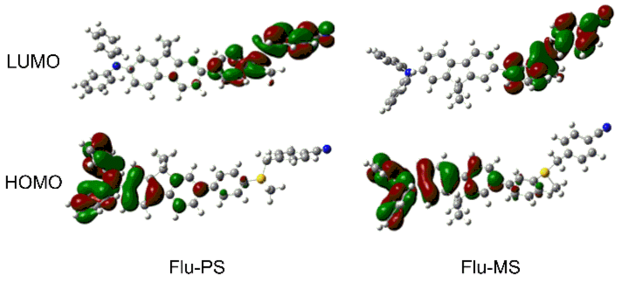

Fig. 2 By Ming JIN et al.

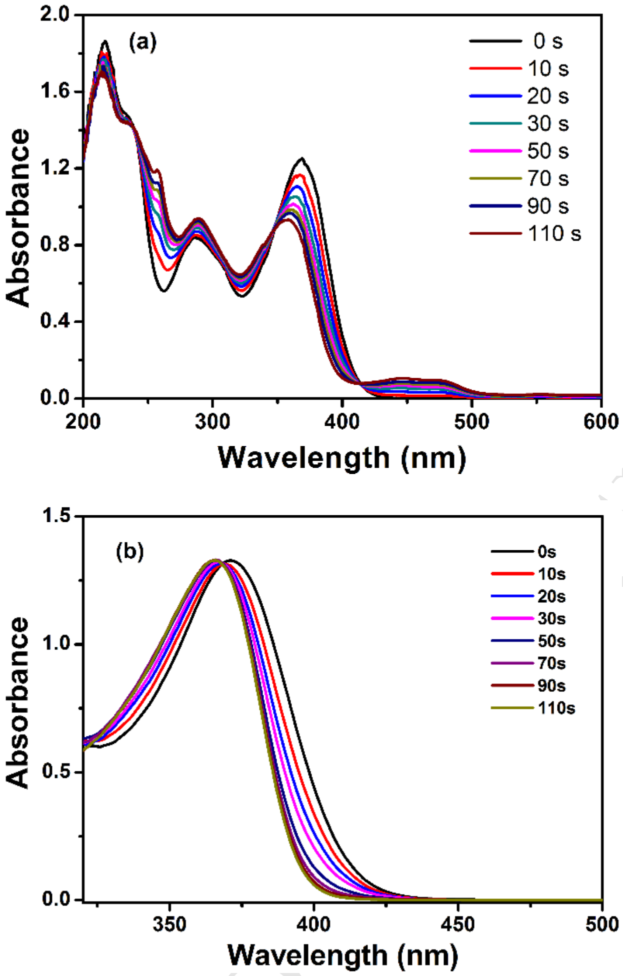

Fig. 3 By Ming JIN et al.

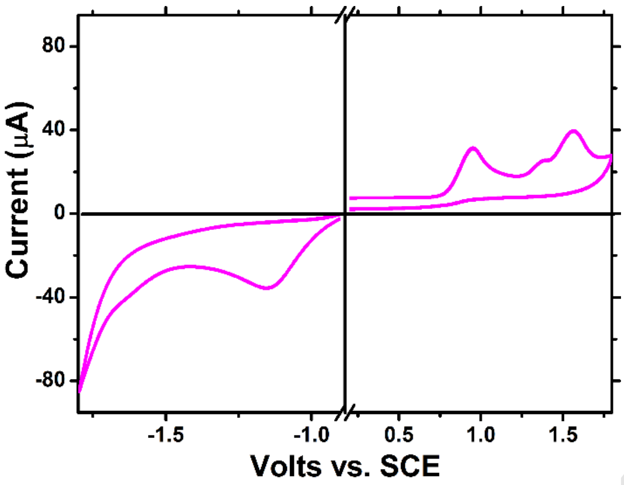

Fig. 4 By Ming JIN et al.

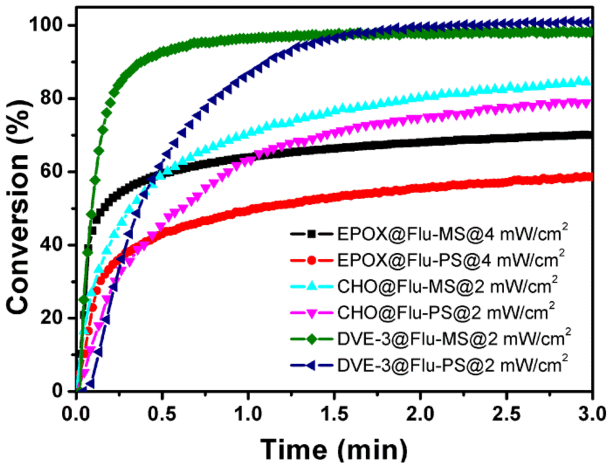

Fig. 5 By Ming JIN et al.

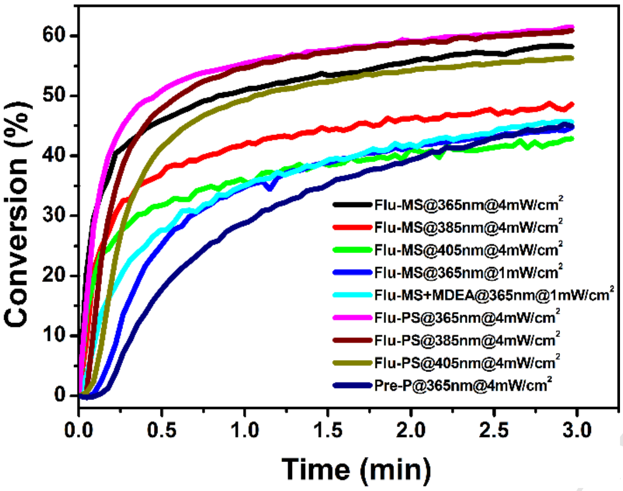

Fig. 6 By Ming JIN et al.

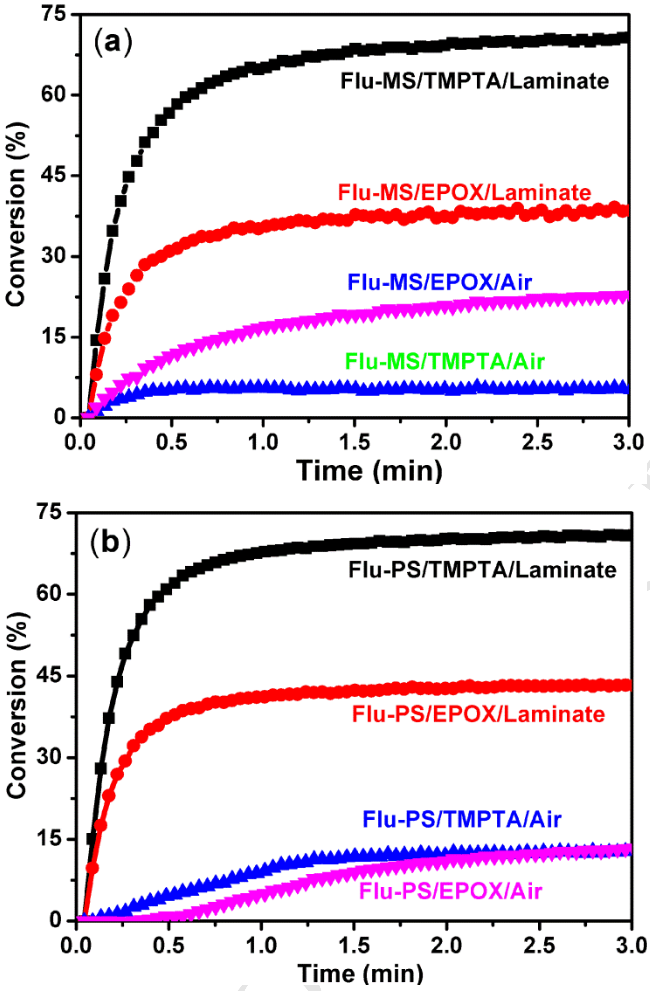

Fig. 7 By Ming JIN et al.

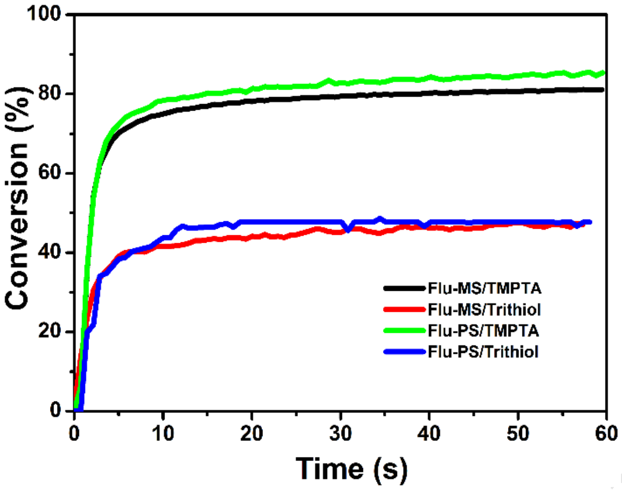

Fig. 8 By Ming JIN et al.

Table 1 Summary of optical data and electrochemical parameters for Flu-PS and Flu-MS.

PAGs	λ_{abs} (nm)[a]	ε_{max}(M^{-1} cm^{-1})[a]	E_{00} (eV)	E_{ox} (V)[b]	E_{red} (V)[b]	ΔG (kJ mol^{-1})[c]	Φ_{H^+}[d]
Flu-MS	368	36,900	3.02	0.75	-1.1	-111.61	0.63
Flu-PS	378	39,400	2.88	0.88	-1.2	-71.92	0.43

[a] In acetonitrile, and the error is approximately 10%; [b] vs. aqueous SCE in ACN (considering $E_{Fc/Fc+}$ = 0.53 V in ACN *vs.* aqueous SCE); [c] free energy change calculated from eq (1); and [d] measured at 365 nm, and the error is approximately 15%.

Table 2 Light absorption properties of sulfoniums and their molar extinction coefficients (ε in M^{-1} cm^{-1}) at the maximum emission wavelengths of different LEDs.

Sulfonium	λ_{abs}(nm)	ε_{max}	$\varepsilon_{365\ nm}$[a]	$\varepsilon_{385\ nm}$[a]	$\varepsilon_{405\ nm}$[a]	ε_{450nm}[a]
Flu-MS	368	36,900	36,700	24,300	5600	100
Flu-PS	378	39,400	35,000	37,700	22,000	900

[a] For different Near UV/visible LEDs.

Table 3 DVE-3, CHO, EPOX, TMPTA, TMPTA/EPOX and TMPTA/Trithiol conversions obtained with 365 nm LED illumination in the presence of Flu-MS or Flu-PS (1 wt%).

Monomers	PIs	Intensity (mW cm^{-2})	Conversion (%)
DVE-3	Flu-MS	2	98.0
DVE-3	Flu-PS	2	99.0
CHO	Flu-MS	2	84.5
CHO	Flu-PS	2	78.9
EPOX	Flu-MS	4	70.0
EPOX	Flu-PS	4	58.6
TMPTA	Flu-MS	4	58.2
TMPTA	Flu-PS	4	61.4
EPOX/TMPTA	Flu-MS	2	38.6/70.7
EPOX/TMPTA	Flu-PS	2	43.2/70.8
Trithiol/TMPTA	Flu-MS	2	49.7/82.4
Trithiol/TMPTA	Flu-PS	2	47.3/85.4

Highlights:

1) High efficiency: the introduction of fluorenyl group in PAGs enhances the Φ_H^+.

2) Energy saving: the LEDs' intensities in the range of 1-4 mW/cm^2 are enough.

3) Multifunction: One-component photoinitiator for versatile photopolymerizations.